

Accepted Manuscript

Deposited zirconocene chloride on silica-layered CuFe_2O_4 as a highly efficient and reusable magnetically nanocatalyst for one-pot Suzuki-Miyaura coupling reaction

Behzad Zeynizadeh, Farhad Sepehraddin



PII: S0022-328X(17)30731-3

DOI: [10.1016/j.jorganchem.2017.12.033](https://doi.org/10.1016/j.jorganchem.2017.12.033)

Reference: JOM 20228

To appear in: *Journal of Organometallic Chemistry*

Received Date: 2 October 2017

Revised Date: 8 December 2017

Accepted Date: 26 December 2017

Please cite this article as: B. Zeynizadeh, F. Sepehraddin, Deposited zirconocene chloride on silica-layered CuFe_2O_4 as a highly efficient and reusable magnetically nanocatalyst for one-pot Suzuki-Miyaura coupling reaction, *Journal of Organometallic Chemistry* (2018), doi: 10.1016/j.jorganchem.2017.12.033.

This is a PDF file of an unedited manuscript that has been accepted for publication. As a service to our customers we are providing this early version of the manuscript. The manuscript will undergo copyediting, typesetting, and review of the resulting proof before it is published in its final form. Please note that during the production process errors may be discovered which could affect the content, and all legal disclaimers that apply to the journal pertain.

Deposited Zirconocene Chloride on Silica-Layered CuFe₂O₄ as a Highly Efficient and Reusable Magnetically Nanocatalyst for One-Pot Suzuki-Miyaura Coupling Reaction

Behzad Zeynizadeh and Farhad Sepehraddin*

Faculty of Chemistry, Urmia University, Urmia 5756151818, Iran
farhad.sepehraddin@gmail.com**Abstract:**

The novel core-shell magnetically nanoparticles of CuFe₂O₄@SiO₂@ZrCp₂Cl_x (x: 0–2) were synthesized and used as a highly efficient catalyst for Suzuki-Miyaura coupling reaction of various aryl halides with phenylboronic acid. The reactions were carried out in PEG-400 (70 °C) to afford biaryls in high to excellent yields. The core-shell nanocomposite was easily separated from the reaction by an external magnet and reused for 5 times without significant loss of its catalytic activity. Characterization of the zirconocene nanocomposite was carried out by FT-IR, SEM, EDX, XRD, ICP-OES, AGFM, TGA and BET analyses.

Keywords: Aryl halides, Biaryls, C-C coupling, Cp₂ZrCl₂, PhB(OH)₂, Suzuki-Miyaura

1. Introduction

In recent years, synthesis and application of reusable heterogeneous catalysts especially immobilization of diverse homogeneous catalysts on the core of nanomagnetic materials has attracted a great deal of attentions [1–5]. The main advantage of this protocol is here that the prepared nanocomposites can be easily removed from the reaction by a simple magnetic decantation. In addition, this type of nanocatalysts possesses high surface area and accelerates the rate of reactions dramatically [6, 7].

In a past decade, various transition metals such as Pd [8], Ni [9], Zn [10], Cu [11], Ru [12], Co [13], Au [14], Fe [15] and Pd/ZrO₂ [16] have been widely used for many types of coupling reactions. The reaction of C-C bond coupling has been frequently employed for synthesis of agrochemicals, pharmaceuticals, biologically active compounds, polymers, liquid crystals and advanced materials [17–20]. In this context, Suzuki-Miyaura coupling reaction is one of the most important synthetic routes for the preparation of various biaryls [21–23].

In line with the outlined strategies, herein, we wish to report a synthesis of novel deposited zirconocene chloride on silica-layered copper ferrite, CuFe₂O₄@SiO₂@ZrCp₂Cl_x (x: 0–2), as a highly efficient magnetically nanocatalyst for one-pot C-C bond coupling of various aryl halides with phenylboronic acid in PEG-400 (70 °C).

2. Experimental**2.1. Materials and instruments**

All reagents and solvents were purchased from commercial sources and used without further purification. ¹H, ¹³C NMR and FT-IR spectra were recorded on Bruker Avance 250/400 MHz and Bruker Vertex 70 FT-IR spectrometers. Mass spectra were recorded on Agilent-5975C inert XL MSD operating at ionization potential of 70 eV. Melting points were measured by Electrothermal 9100 apparatus. Thermogravimetric analysis (TGA) was carried out on Shimadzu DTG-60 instrument. Size and morphology of particle was determined using FESEM–TESCAN MIRA3 instrument. Powder XRD was obtained by an X'PertPro Panalytical, Holland diffractometer in 40 kV and 30 mA with a CuK α radiation ($\lambda=1.5418$ Å), and the diffraction patterns were recorded in 2 θ range (10–80°). Elemental analysis of Zr was carried out by inductively coupled plasma-optical emission spectrometry (ICP-OES) model ARCOS, Germany. The N₂ absorption-desorption isotherms were recorded on Belsorp-max instrument. The specific surface area of samples was determined using Brunauer-Emmett-Teller (BET) method. The pore volume and pore size distribution were obtained from desorption profile of isotherms using Barrett-Joyner-Halanda (BJH) method. Magnetic properties of nanocomposites were measured on alternating gradient force magnetometer (AGFM, Meghnatis Daghigh Caviar Co., Iran) at room temperature. Ultrasonic irradiation

was carried out in GT SONIC (VGT-1860QTS, China). Thin layer chromatography (TLC) was applied for the purity determination of products and reaction monitoring over gel SILG/UV 254 aluminum plates.

2.2 Preparation of $\text{CuFe}_2\text{O}_4@ \text{SiO}_2@ \text{ZrCp}_2\text{Cl}_x$ (x: 0-2) MNPs

Synthesis of $\text{CuFe}_2\text{O}_4@ \text{SiO}_2@ \text{ZrCp}_2\text{Cl}_x$ (x: 0–2) MNPs was carried out in a three-step procedure: At first, magnetically nanoparticles of CuFe_2O_4 were prepared through a chemical co-precipitation protocol [24] as following:

$\text{FeCl}_3 \cdot 6\text{H}_2\text{O}$ (2.216 g, 8.2 mmol) and $\text{CuCl}_2 \cdot 2\text{H}_2\text{O}$ (0.699 g, 4.1 mmol) were dissolved in deionized water (75 mL) and stirred at room temperature under nitrogen atmosphere. After few minutes, a basic solution of NaOH (3 g in 15 mL H_2O) was drop-wisely added to the prepared solution of iron and copper chlorides in 10 min and was continued to stirring vigorously. In a meanwhile of NaOH addition, fine brown-black particles of CuFe_2O_4 were precipitated. The resulting mixture was heated on an oil bath (90 °C) for 5 h. After cooling to the room temperature, the precipitate was separated by an external magnet and washed with deionized water (30 mL) and ethanol (20 mL), and was then dried at 80 °C for 12 h. The obtained CuFe_2O_4 MNPs was calcinated at 700 °C for 5 h.

At the second step, the obtained CuFe_2O_4 MNPs (2 g) were dispersed in a mixture of $\text{EtOH-H}_2\text{O-25\%}$ aqueous NH_3 (50:20:10 mL, respectively) by sonication. Afterward, PEG-400 (3.36 g) and then tetraethyl orthosilicate (2 mL) was added to the prepared suspension of CuFe_2O_4 under vigorous stirring. The mixture was then stirred for 38 h at room temperature. Magnetically nanoparticles of $\text{CuFe}_2\text{O}_4@ \text{SiO}_2$ were isolated with an external magnet and washed with ethanol and deionized water and then dried at room temperature [25].

Subsequently, a suspension of $\text{CuFe}_2\text{O}_4@ \text{SiO}_2$ (1 g) in *n*-hexane (50 mL) was prepared and irradiated in an ultrasonic bath for 30 min under nitrogen atmosphere. To this mixture, a solution of Cp_2ZrCl_2 (1 g) in *n*-hexane (50 mL) was added and the resulting mixture was stirred for 10 h under reflux and nitrogen atmosphere. The prepared magnetically nanoparticles of $\text{CuFe}_2\text{O}_4@ \text{SiO}_2@ \text{ZrCp}_2\text{Cl}_x$ (x: 0–2) were separated by a simple magnetic decantation and washed with ethanol and deionized water to remove the residual contaminants. The obtained nanoparticles were then dried under vacuum at room temperature to afford the final nanocomposite material (1.76 g).

2.3 A general procedure for C-C bond coupling of aryl halides with phenylboronic acid

In a round-bottom flask (10 mL), a mixture of aryl halide (1 mmol), phenylboronic acid (1 mmol), K_2CO_3 (1.5 mmol) and $\text{CuFe}_2\text{O}_4@ \text{SiO}_2@ \text{ZrCp}_2\text{Cl}_x$ (x: 0–2) (5 mg) in PEG-400 (2 mL) was prepared and the mixture was continued to stirring in oil bath (70 °C) for an appropriate time (Table 3). After completion of the reaction (monitored by TLC), the nanocatalyst was separated by an external magnet. Distilled water (5 mL) was then added and the mixture was stirred for additional 5 min. The product was extracted with EtOAc (3 × 5 mL) and the organic layer was then dried over anhydrous Na_2SO_4 . Evaporation of the solvent under reduced pressure affords the crude biaryl product following with a further purification by a short column chromatography on silica gel (eluent, *n*-hexane: EtOAc / 7:3).

2.4 Selected spectral data

Biphenyl (Table 3, entry 1)

White solid, m.p. 68–69 °C, ^1H NMR (250 MHz, CDCl_3): δ (ppm) 7.36–7.39 (m, 2H), 7.46–7.52 (m, 4H), 7.64 (d, $J = 7.5$ Hz, 4H); EI-MS (70 eV): m/z (%) = 154 (M^+ , 100).

2-Methylbiphenyl (Table 3, entry 5)

Colorless oil, b.p. 255.5 °C/760 mmHg, ^1H NMR (250 MHz, CDCl_3): δ (ppm) 2.46 (s, 3H), 7.25–7.57 (m, 9H); EI-MS (70 eV): m/z : 168 (M^+ , 100).

4-Cyanobiphenyl (Table 3, entry 7)

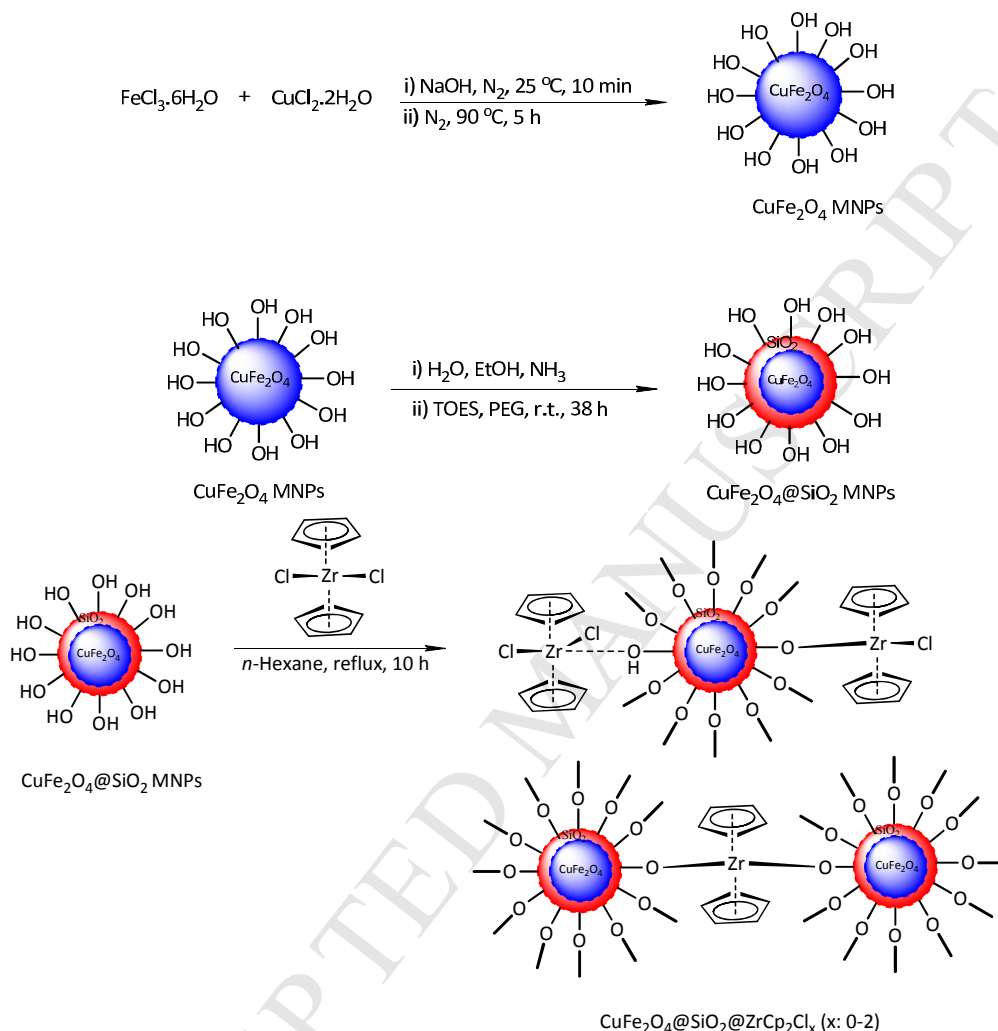
White solid, m.p. 85–87 °C, ^1H NMR (400 MHz, CDCl_3): δ (ppm) 7.77–7.73 (m, 2H), 7.72–7.70 (m, 2H), 7.64–7.61 (m, 2H), 7.54–7.50 (m, 2H), 7.50–7.44 (m, 1H)

4-Nitrobiphenyl (Table 3, entry 8)

Yellow solid, m.p. 111–114 °C, ^1H NMR (400 MHz, CDCl_3): δ (ppm) 8.35–8.32 (m, 2H), 7.79–7.75 (m, 2H), 7.67–7.64 (m, 2H), 7.56–7.46 (m, 2H), 7.46–7.29 (m, 1H)

3. Results and discussion

The study was started by synthesis of novel magnetically nanoparticles of $\text{CuFe}_2\text{O}_4@ \text{SiO}_2@ \text{ZrCp}_2\text{Cl}_x$ (x : 0–2) through a depicted three-step procedure in Scheme 1:



Scheme 1. Synthesis of $\text{CuFe}_2\text{O}_4@ \text{SiO}_2@ \text{ZrCp}_2\text{Cl}_x$ (x : 0–2) MNPs

The scheme shows that magnetically nanoparticles of CuFe_2O_4 were initially prepared by chemical co-precipitation of $\text{FeCl}_3 \cdot 6\text{H}_2\text{O}$ and $\text{CuCl}_2 \cdot 2\text{H}_2\text{O}$ in aqueous NaOH [24]. So, the prepared nanocores of CuFe_2O_4 were coated with silica layer using tetraethyl orthosilicate. Through the functionalization of $\text{CuFe}_2\text{O}_4@ \text{SiO}_2$ MNPs with zirconocene dichloride, magnetically nanoparticles of $\text{CuFe}_2\text{O}_4@ \text{SiO}_2@ \text{ZrCp}_2\text{Cl}_x$ (x : 0–2) was finally synthesized. The prepared core-shell zirconocene nanocomposite was then characterized by FT-IR, SEM, EDX, XRD, ICP-OES, AGFM, TGA and BET analyses.

3.1. Characterization of $\text{CuFe}_2\text{O}_4@ \text{SiO}_2@ \text{ZrCp}_2\text{Cl}_x$ (x : 0–2) MNPs

Thermogravimetric analysis (TGA) of $\text{CuFe}_2\text{O}_4@ \text{SiO}_2@ \text{ZrCp}_2\text{Cl}_x$ MNPs was shown in Figure 1. Through the analysis, mass losing of the nanocomposite through dehydration, removing of organic moiety or fragmentation was studied at a programmable heating. The recorded plot for zirconocene nanocomposite shows a weight loss in the region of r.t.–200 °C via dehydration of adsorbed water or surface hydroxyl groups. By fragmentation and removing of organic moiety, a second weight loss at 200–600 °C was also observed in thermogravimetric curve of the nanocomposite.

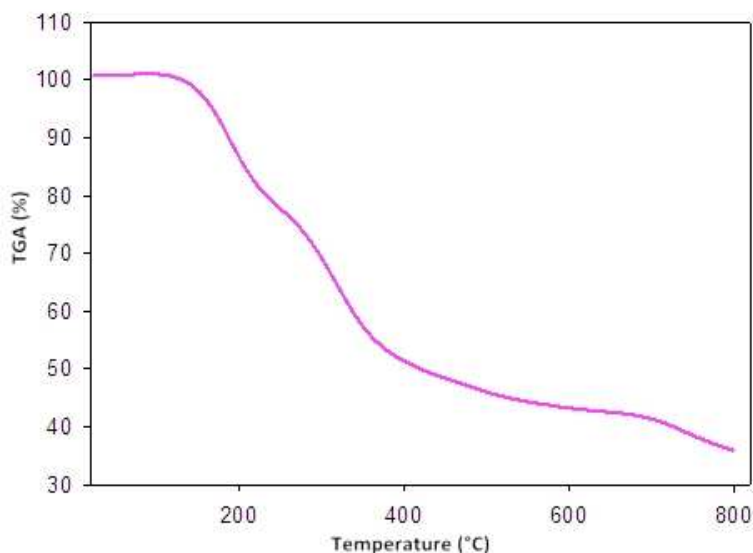


Fig. 1. TGA analysis of $\text{CuFe}_2\text{O}_4@SiO_2@ZrCp_2Cl_x$ ($x: 0-2$) MNPs

Figure 2 shows the recorded FT-IR spectra for CuFe_2O_4 and $\text{CuFe}_2\text{O}_4@SiO_2@ZrCp_2Cl_x$ ($x: 0-2$) MNPs. Both of spectrum 2a and 2b show the stretching vibration bands at 410 and 580 cm^{-1} attributed to the bonding of Cu-O and Fe-O, respectively, and a broad absorbance around 3400 cm^{-1} due to stretching vibration of surface hydroxyl groups. Presence of silica layer on the surface of copper ferrite nanoparticles is confirmed by the absorbance at 1150 cm^{-1} showing Si-O and 1620 cm^{-1} showing C=C stretching vibration of Cp groups (Fig. 2b). These results demonstrated that zirconocene chloride was successfully immobilized on the surface of $\text{CuFe}_2\text{O}_4@SiO_2$ MNPs.

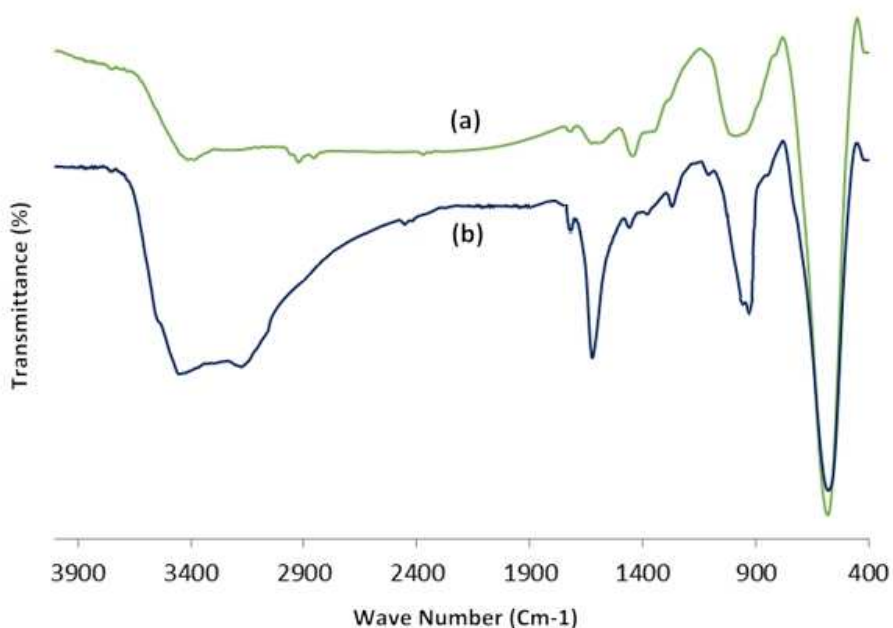


Fig. 2. FT-IR spectrum of a) CuFe_2O_4 and b) $\text{CuFe}_2\text{O}_4@SiO_2@ZrCp_2Cl_x$ ($x: 0-2$) MNPs

The morphology and size distribution of particles in CuFe_2O_4 and $\text{CuFe}_2\text{O}_4@SiO_2@ZrCp_2Cl_x$ ($x: 0-2$) MNPs are illustrated in Figure 3. The SEM images show that in both of materials, the nanoparticles have uniform shapes. SEM analysis exhibited that size of nanoparticles in CuFe_2O_4 and $\text{CuFe}_2\text{O}_4@SiO_2@ZrCp_2Cl_x$ ($x: 0-2$) MNPs is varied from $15-20$ and $30-35\text{ nm}$, respectively. By EDX analysis, elemental composition of Cu, Fe, O, Cl, Si, and Zr in $\text{CuFe}_2\text{O}_4@SiO_2@ZrCp_2Cl_x$ ($x: 0-2$) MNPs was also demonstrated (Figure 4).

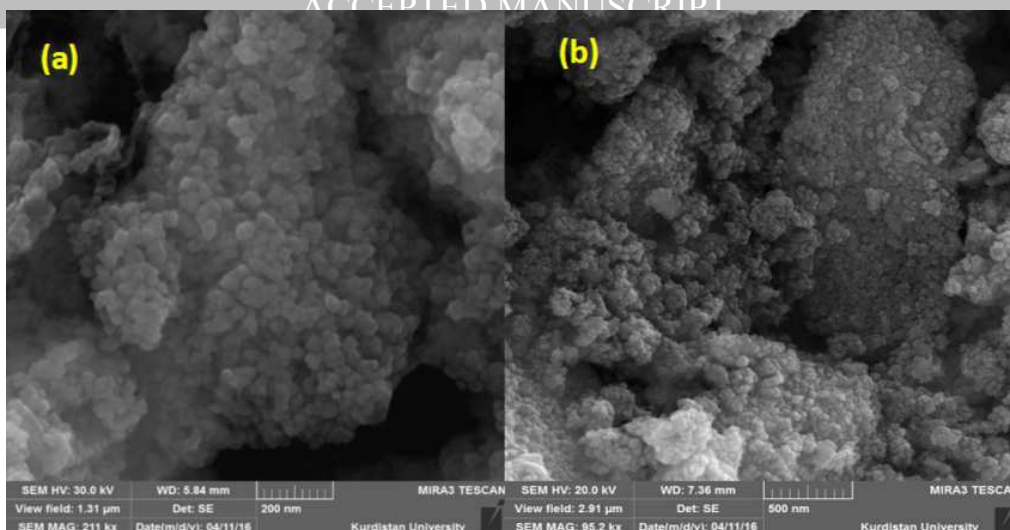


Fig. 3. SEM images of a) CuFe_2O_4 and b) $\text{CuFe}_2\text{O}_4@\text{SiO}_2@\text{ZrCp}_2\text{Cl}_x$ ($x: 0-2$) MNPs

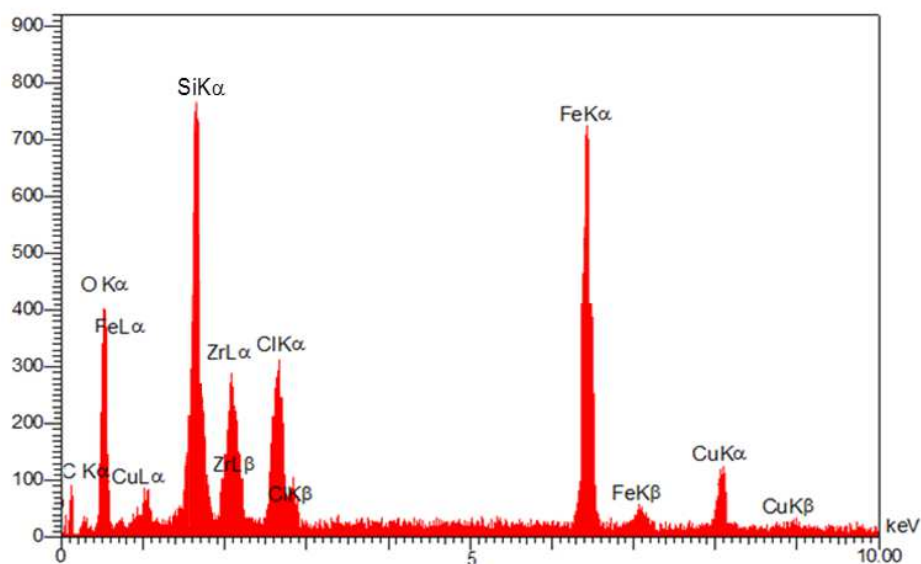


Fig. 4. EDX analysis of $\text{CuFe}_2\text{O}_4@\text{SiO}_2@\text{ZrCp}_2\text{Cl}_x$ ($x: 0-2$) MNPs

The amount of Zr (4.72%) in $\text{CuFe}_2\text{O}_4@\text{SiO}_2@\text{ZrCp}_2\text{Cl}_x$ ($x: 0-2$) MNPs was determined successfully by ICP-OES (inductively coupled plasma optical emission spectrometry) technique.

X-ray diffraction pattern of $\text{CuFe}_2\text{O}_4@\text{SiO}_2@\text{ZrCp}_2\text{Cl}_x$ ($x: 0-2$) nanoparticles was shown in Figure 5. In this pattern, the phase of nanoparticle is identified by the peak position of 19° (101), 30° (112), 35° (211), 37° (202), 42° (220), 52° (312), 57° (321), 63° (224), 67° (400), 74° (420), 75° (413) and 77° (422) which is in consistent with the standard XRD pattern of CuFe_2O_4 (JCPDS 77-0010). This observation illustrated that during the immobilization of ZrCp_2Cl_2 , the crystalline structure of CuFe_2O_4 was remained intact [24].

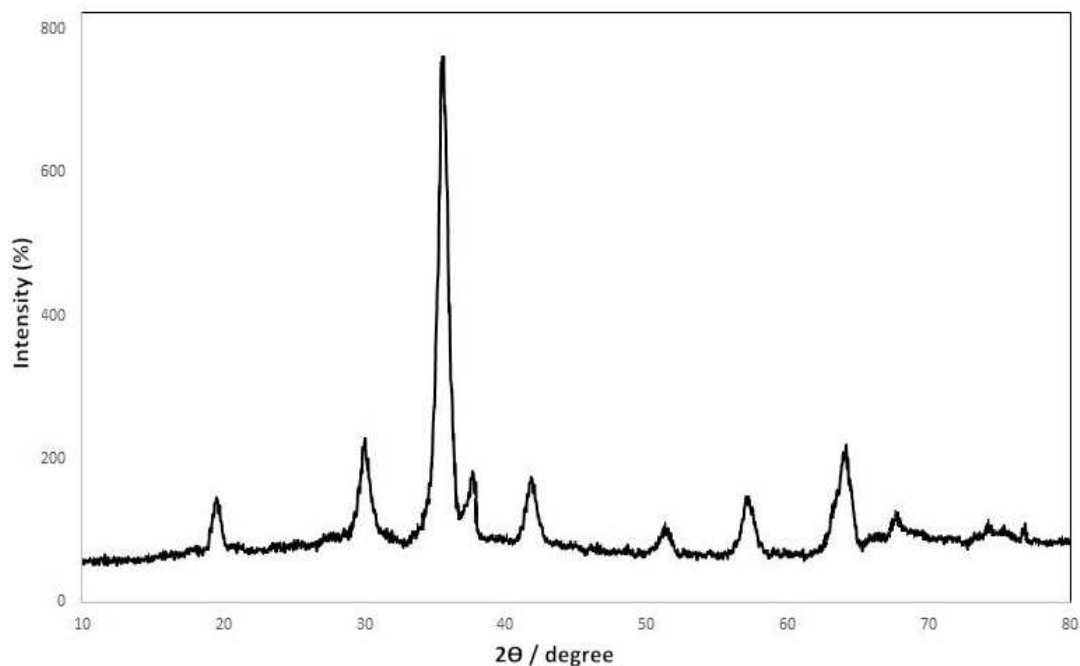


Fig. 5. XRD pattern of $\text{CuFe}_2\text{O}_4@SiO_2@ZrCp_2Cl_x$ ($x: 0-2$) MNPs

Figure 6 shows N_2 adsorption-desorption isotherms of $\text{CuFe}_2\text{O}_4@SiO_2$ and $\text{CuFe}_2\text{O}_4@SiO_2@ZrCp_2Cl_x$ ($x: 0-2$) MNPs. Based on these isotherms, the calculated BET specific surface area (S_{BET}) and total pore volumes (V_{total}) are summarized in Table 1. Observation of the results shows that the presence of $ZrCp_2Cl_x$ moieties on the surface of $\text{CuFe}_2\text{O}_4@SiO_2$ decreases S_{BET} and increases V_{total} values.

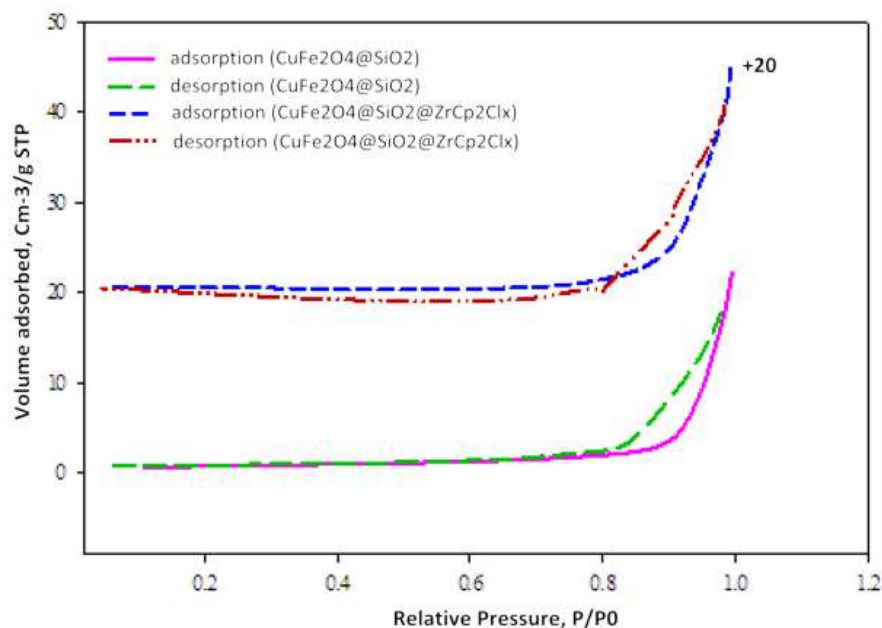


Fig. 6. N_2 adsorption-desorption isotherm for $\text{CuFe}_2\text{O}_4@SiO_2$ and $\text{CuFe}_2\text{O}_4@SiO_2@ZrCp_2Cl_x$ ($x: 0-2$) MNPs

Table 1. The obtained parameters from N_2 adsorption-desorption isotherms		
Sample	S_{BET} (m^2/g)	V_{total} (Cm^3/g)
$\text{CuFe}_2\text{O}_4@SiO_2$	2.762	0.031
$\text{CuFe}_2\text{O}_4@SiO_2@ZrCp_2Cl_x$ ($x: 0-2$)	1.787	0.036

Magnetic susceptibility of CuFe_2O_4 and $\text{CuFe}_2\text{O}_4@SiO_2@ZrCp_2Cl_x$ ($x: 0-2$) MNPs was also studied by obtaining the specific saturation magnetization (M_s), remanent magnetism (M_r) and coercivity field (H_c) of

the nanoparticles. The plot of saturation magnetization (M_s) versus coercivity field (H_c) for examined nanomagnetic materials clearly shows ferromagnetic behavior of CuFe_2O_4 . M_s , M_r and H_c values for CuFe_2O_4 are about 0.03, 0.002 a.u. and 100 Oe, respectively (Figure 7). At the same field, the values for $\text{CuFe}_2\text{O}_4@SiO_2@ZrCp_2Cl_x$ (x : 0–2) are about 0.007, 0.001 a.u. and 0 Oe, respectively. These nanoparticles easily separated by using an external magnet.

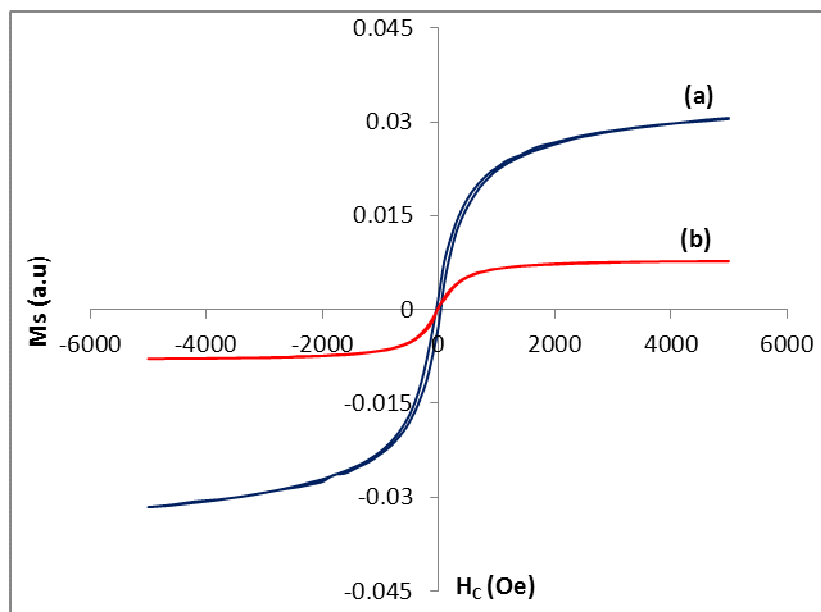


Fig. 7. Magnetization curve of a) CuFe_2O_4 and b) $\text{CuFe}_2\text{O}_4@SiO_2@ZrCp_2Cl_x$ (x : 0–2) MNPs at r.t.

3.2. Catalytic activity of $\text{CuFe}_2\text{O}_4@SiO_2@ZrCp_2Cl_x$ (x : 0–2) MNPs for C-C bond coupling

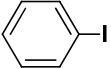
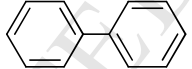
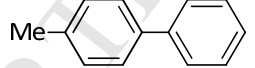
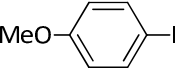
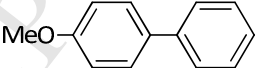
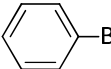
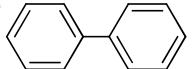
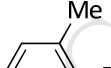
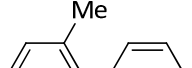
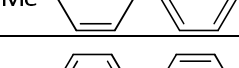
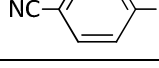
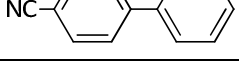
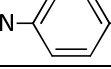
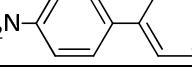
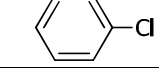
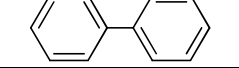
After synthesis and characterization of $\text{CuFe}_2\text{O}_4@SiO_2@ZrCp_2Cl_x$ (x : 0–2) MNPs, the catalytic activity of this nanocomposite was examined in Suzuki-Miyaura C-C bond coupling of aryl halides with phenylboronic acid. Reaction conditions were optimized by performing the coupling reaction of iodobenzene with phenylboronic acid in the presence of $\text{CuFe}_2\text{O}_4@SiO_2@ZrCp_2Cl_x$ (x : 0–2) MNPs using various solvents, bases, varying the amounts of nanocatalyst as well as temperature of the reaction. The results of these investigations are summarized in Table 2.

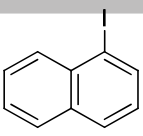
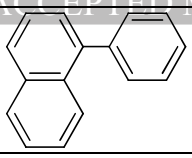
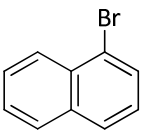
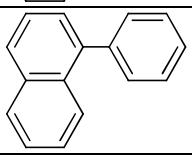
Table 2. Optimization experiments for C-C bond coupling of PhI with PhB(OH)_2						
Entry	Zr-cat. (mg)	Solvent	Base	Temp. (°C)	Time (min)	Yield (%) ^b
1	–	PEG-400	K_2CO_3	120	180	–
2	3	PEG-400	K_2CO_3	70	75	86
3	5	PEG-400	K_2CO_3	70	30	98
4	7	PEG-400	K_2CO_3	70	25	98
5	5	PEG-400	K_2CO_3	rt	300	84
6	5	EtOH	K_2CO_3	70	150	69
7	5	EtOAc	K_2CO_3	60	160	73
8	5	CH_2Cl_2	K_2CO_3	60	120	69
9	5	H_2O	K_2CO_3	70	200	70
10	5	DMF	K_2CO_3	70	35	95
11	5	PEG-400	Et_3N	70	140	60
12	5	PEG-400	$n\text{-Pr}_3\text{N}$	70	190	62
13	5	PEG-400	KOH	70	45	70

^a All reactions were carried out with the molar ratio of PhI: PhB(OH)_2 :Base (1:1:1.5). ^b Isolated yield.

Observation of the results reveals that the influence of nanocatalyst on the rate of coupling reaction is noteworthy. Entry 1 shows that performing of the model reaction in the absence of nanocatalyst did not produce any product. However, using the little amounts of $\text{CuFe}_2\text{O}_4@\text{SiO}_2@\text{ZrCp}_2\text{Cl}_x$ (x : 0–2) MNPs dramatically accelerated the rate of reaction. Carrying out of the coupling reaction inside various solvents and using different amounts of nanocatalyst resulted that completion of the reaction of PhI (1 mmol) with $\text{PhB}(\text{OH})_2$ (1 mmol) requires 5 mg $\text{CuFe}_2\text{O}_4@\text{SiO}_2@\text{ZrCp}_2\text{Cl}_x$ (x : 0–2) MNPs and 1.5 mmol K_2CO_3 in PEG-400 (70 °C) as the optimum reaction conditions (Entry 3). In order to determine the influence of Zr moiety on Suzuki-Miyaura bond coupling reaction, we also performed the model reaction in the presence of CuFe_2O_4 and $\text{CuFe}_2\text{O}_4@\text{SiO}_2$ MNPs at the optimized reaction conditions. Investigation of the results showed that the progress of the reactions was poor (25–30%) and did not exhibit any impressive results. At the next, the capability of $\text{CuFe}_2\text{O}_4@\text{SiO}_2@\text{ZrCp}_2\text{Cl}_x$ (x : 0–2) MNPs was further studied by performing C-C bond coupling of diverse aryl halides with phenylboronic acid at the optimized reaction conditions. The results of this investigation are illustrated in Table 3. As seen, all reactions were carried out successfully to afford biaryl products in high to excellent yields within 10–100 min. The table also exhibited that aryl halides containing electron-withdrawing groups has higher rate enhancement in comparison to those containing electron-releasing groups (Table 3, entries 6 and 8). Moreover, the obtained results for coupling reaction of aryl bromides and chlorides with $\text{PhB}(\text{OH})_2$ reveals that the present protocol was also efficient and produced the corresponding biaryls in high yields (entries 4–12). As it is anticipated, the reactivity of aryl iodides was higher than their bromide and chloride derivatives.

Table 3. C-C bond coupling of aryl halides with phenylboronic acid in the presence of $\text{CuFe}_2\text{O}_4@\text{SiO}_2@\text{ZrCp}_2\text{Cl}_x$ (x : 0–2) MNPs ^a

$\text{Ar-X} + \text{PhB}(\text{OH})_2 \xrightarrow[\text{K}_2\text{CO}_3, \text{PEG-400}, 70^\circ\text{C}]{\text{CuFe}_2\text{O}_4@\text{SiO}_2@\text{ZrCp}_2\text{Cl}_x (5 \text{ mg})} \text{Ar-Ph}$ X: I, Br, Cl					
Entry	ArX	Product	Time (min)	Yield (%) ^b	Mp (°C) [Ref.]
1			30	98	68–69 [26]
2			50	96	45–47 [27]
3			80	89	86–89 [28]
4			40	97	68–69 [26]
5			90	87	255.5/760 mmHg [27]
6			55	87	45–47 [29]
7			15	97	85–87 [26]
8			10	98	111–114 [29]
9			100	70	68–69 [26]
10			30	92	111–114 [29]

11			75	90	324–325/760 mmHg [30]
12			85	88	324–325/760 mmHg [30]

^aAll reactions were carried out with the molar ratio of ArX:PhB(OH)₂:K₂CO₃ (1:1:1.5) in the presence of CuFe₂O₄@SiO₂@ZrCp₂Cl_x (5 mg) in PEG-400 (2 mL) at 70 °C. ^b Isolated yield.

3.3. Recycling of CuFe₂O₄@SiO₂@ZrCp₂Cl_x (x: 0-2) MNPs

Reusability of the nanocatalyst was studied by performing C-C bond coupling of PhI with PhB(OH)₂ in the presence of recycled CuFe₂O₄@SiO₂@ZrCp₂Cl_x (x: 0–2) MNPs. After completion of the reaction at the first run, the catalyst was recovered by an external magnet, washed with ethyl acetate, dried in an oven and then reused for the next run of the coupling reaction. Figure 8 shows the yield of five consecutive cycles of biphenyl synthesis through the coupling reaction of phenyl iodide with phenylboronic acid in the presence of recycled Zr-nanocomposite. After five recycling and reusing the nanocatalyst, ICP-OES analysis showed that the amount of Zr was 4.71%. This result obviously indicates that the activity of nanocatalyst was remained intact during the recycling process.

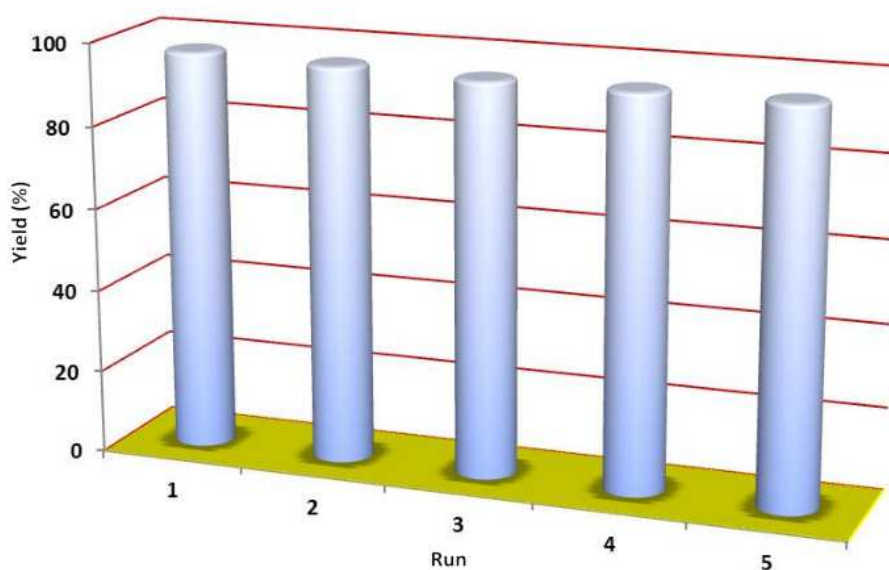


Fig. 8. Reusability of CuFe₂O₄@SiO₂@ZrCp₂Cl_x (x: 0–2) MNPs

4. Conclusions

In this study, the immobilization of zirconocene chloride on silica-layered copper ferrite as a novel core-shell Zr-based nanocomposite, CuFe₂O₄@SiO₂@ZrCp₂Cl_x (x: 0–2), was carried out successfully. The nanocatalyst was characterized by FT-IR, SEM, EDX, XRD, ICP-OES, AGFM, TGA and BET analyses. The prepared core-shell zirconocene MNPs exhibited an excellent catalytic activity and reusability towards C-C bond coupling of diverse aryl halides with phenylboronic acid. All reactions were carried out in the presence of 5 mg of the nanocatalyst using K₂CO₃ in PEG-400 at 70 °C. The nanocatalyst was used at least for 5 catalytic cycles without significant loss of its catalytic activity. Remarkable reusability and easy separation of the catalyst, first application of zirconium in Suzuki-Miyaura C-C bond coupling reaction, high yields and mild

basic reaction conditions as well as the benefits of using PEG-400 as a green solvent are the advantages which make this protocol a perfect choice for the titled transformation.

5. Acknowledgements

The authors gratefully appreciated the financial support of this work by the research council of Urmia University.

6. References

1. J. H. Clark and C. N. Rhodes, *Clean Synthesis Using Porous Inorganic Solid Catalysts and Supported Reagents*, Royal Society of Chemistry, Cambridge, 2000.
2. G. V. Smith and F. Notheisz, *Heterogeneous Catalysis in Organic Chemistry*, Academic Press, San Diego, CA, 1999.
3. M. Zeinali-Dastmalbaf, A. Davoodnia, M. M. Heravi, N. Tavakoli-Hoseini, A. Khojastehnezhad and H. A. Zamani, *Bull. Korean Chem. Soc.* 32 (2011) 656–658.
4. G. Lv, W. Mai, R. Jin and L. Gao, *Synlett* (2008) 1418–1422.
5. T. J. Yoon, W. Lee, Y. S. Oh and J. K. Lee, *New J. Chem.* 27 (2003) 227–229.
6. M. Kooti and M. Afshari, *Mater. Res. Bull.* 47 (2012) 3473–3478.
7. M. Zhu and G. Diao, *J. Phys. Chem. C.* 115 (2011) 24743–24749.
8. A. Rahimi and A. Schmidt, *Synlett* (2010) 1327–1330.
9. S. Z. Tasker, E. A. Standley and T. F. Jamison, *Nature* 509 (2014) 299–309.
10. S. Mata, J. González, R. Vicente and L. A. López, *Eur. J. Org. Chem.* (2016) 2681–2687.
11. A. S. Demir, O. Reis and M. Emrullahoglu, *J. Org. Chem.* 68 (2003) 10130–10134.
12. F. Kakiuchi, Y. Matsuura, S. Kan and N. Chatani, *J. Am. Chem. Soc.* 127 (2005) 5936–5945.
13. L. M. Kumar and B. Ramachandra Bhat, *J. Organomet. Chem.* 827 (2017) 41–48.
14. J. Han, Y. Liu and R. Guo, *J. Am. Chem. Soc.* 131 (2009) 2060–2061.
15. T. Hatakeyama, N. Nakagawa and M. Nakamura, *Org. Lett.* 11 (2009) 4496–4499.
16. A. Monopoli, A. Nacci, V. Calò, F. Ciminale, P. Cotugno, A. Mangone, L. Carla Giannossa, P. Azzone and N. Cioffi, *Molecules* 15 (2010) 4511–4525.
17. N. Miyaura and A. Suzuki, *Chem. Rev.* 95 (1995) 2457–2483.
18. S. Das, S. Bhunia, T. Maity and S. Koner, *J. Mol. Catal. A: Chem.* 394 (2014) 188–197.
19. M. Wen, S. Takakura, K. Fuku, K. Mori and H. Yamashita, *Catal. Today* 242 (2015) 381–385.
20. S. Kazemi Movahed, R. Esmatpoursalmani and A. Bazgir, *RSC Adv.* 4 (2014) 14586–14591.
21. N. Miyaura, T. Yanagi and A. Suzuki, *Synth. Commun.* 11 (1981) 513–519.
22. N. Miyaura, *Cross-Coupling Reactions: A Practical Guide*, Springer-Verlag, Berlin: Heidelberg, 2002.
23. N. T. S. Phan, M. V. Der Sluys and C. W. Jones, *Adv. Synth. Catal.* 348 (2006) 609–679.
24. M. Gholinejad, B. Karimi and F. Mansouri, *J. Mol. Catal. A: Chem.* 386 (2014) 20–27.
25. A. Rostami, A. Ghorbani-Choghamarani, B. Tahmasbi, F. Sharifi, Y. Navasi and D. Moradi, *J. Saudi Chem. Soc.* 21 (2017) 399–407.
26. J. Yang and L. Wang, *Dalton Trans.* 41 (2012) 12031–12037.
27. K. Tanimoro, M. Ueno, K. Takeda, M. Kirihata and S. Tanimori, *J. Org. Chem.* 77 (2012) 7844–7849.
28. M. Cao, Y. Wei, S. Gao and R. Cao, *Catal. Sci. Technol.* 2 (2012) 156–163.
29. P. R. Verma, S. Mandal, P. Gupta and B. Mukhopadhyay, *Tetrahedron Lett.* 54 (2013) 4914–4917.
30. L. Bai and J. X. Wang, *Adv. Synth. Catal.* 350 (2008) 315–320.

Highlights

- Synthesis of magnetically nanoparticles of $\text{CuFe}_2\text{O}_4@ \text{SiO}_2@ \text{ZrCp}_2\text{Cl}_x$
- Bond coupling of aryl halides with $\text{PhB}(\text{OH})_2$ catalyzed by $\text{CuFe}_2\text{O}_4@ \text{SiO}_2@ \text{ZrCp}_2\text{Cl}_x$ MNPs
- Using PEG-400 as a green solvent and K_2CO_3 as a mild base
- Aryl bromides (chlorides) as well as aryl iodides perform the coupling reaction.
- $\text{CuFe}_2\text{O}_4@ \text{SiO}_2@ \text{ZrCp}_2\text{Cl}_x$ MNPs can be reused for 5 catalytic cycles.